Electronic Supplementary Material (ESI) for Lab on a Chip.
This journal is © The Royal Society of Chemistry 2015

Sec. I. Fabrication process for PDMS microfluidic channels with multilayered design[1, 2]

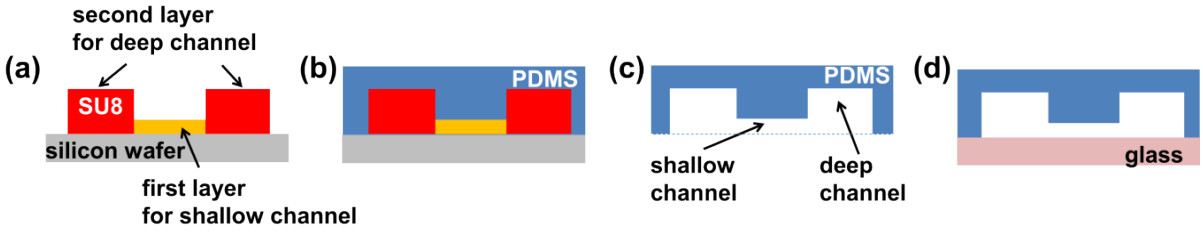

Fig. S1 Scheme of the fabrication process for PDMS microfluidic channels with multilayered design.

This section is followed our previous report.[1, 2] Fig. S1(a) - (d) shows schematic diagrams that describe the procedures for fabricating microfluidic devices with multilayered design. We fabricated microfluidic chips using the standard soft lithography:[1] (a) A 4-inch silicon wafer was spin-coated with negative photoresist (SU-8 2025, MicroChem Inc., target: 25 μm), and then the coated silicon wafer was soft-baked for several minutes. The wafer was exposed under a mask using an aligner and placed on a hot-plate for several minutes of post-exposure baking, followed by a short relaxation time. Post-exposure baking was followed by development at room temperature, after which the whole wafer was rinsed with isopropyl alcohol (IPA) to clean the residues from the wafer. Subsequently, SU-8 2050 was patterned on the first SU-8 layer (target: 50 μm, this layer is for the U-shaped deep channel) with same process as above. (b) A Polydimethylsiloxane (PDMS) precursor (Sylgard 184 Silicone Elastomer, Dow Corning) and a curing agent were mixed at a ratio of 10 to 1, based on weight. Before the PDMS mixture was poured onto the fabricated master, the master was silanized with (tridecafluoro-1,1,2,2,-tetrahydrooctyl)-1-trichlorosilane (Sigma Chemical Co., St. Louis, MO, USA) to allow easier removal of the PDMS after curing. The PDMS mixture was poured onto the master and cured at 95 °C for 1 h. (c) Then, the cured PDMS channel was peeled off from the master, cut and punched to connect microtubes. (d) The PDMS

devices were directly bonded to a glass substrate without any surface treatment and then they were treated with oxygen plasma under 50 sccm of O_2 and 70 W for 40 s (Cute-MP, Femto Science, Korea).

Sec. II. *In situ* formation of nanochannel networks using nanoparticles

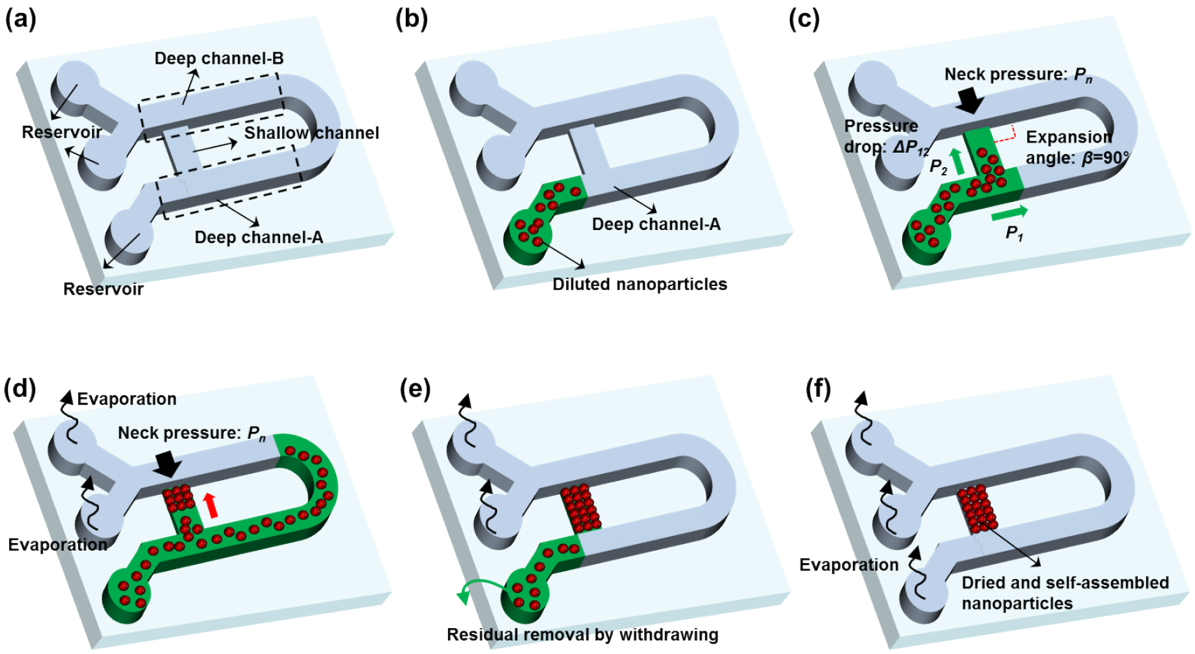

Fig. S2 Fabrication process for the in situ formation of nanochannel networks membrane using the self-assembly of nanoparticles within the PDMS channel.

<Fig. S2(a) and (b)>

(a) The PDMS device with shallow channel and U-shaped deep channels was fabricated as described above. **(b)** In this paper, we used the diameter 240, 300, and 700 nm of silica nanospheres (10 % solids (w/v), Polyscience Inc., USA). Firstly, 100 μL of the diluted nanospheres were centrifuged and re-suspended in 50 μL of the 70 % ethanol (v/v). Finally**,** about 0.1 μL to 0.2 μL of this solution was introduced into the deep channel-A by capillary pressure. Note that too much solution may flow over the deep channel-B across the U-shape microchannel and the neck stop pressure will not work. Therefore, designers should determine the proper volume of the solution as considering the volume of the U-shaped deep channel.

<Fig. S2(c)>

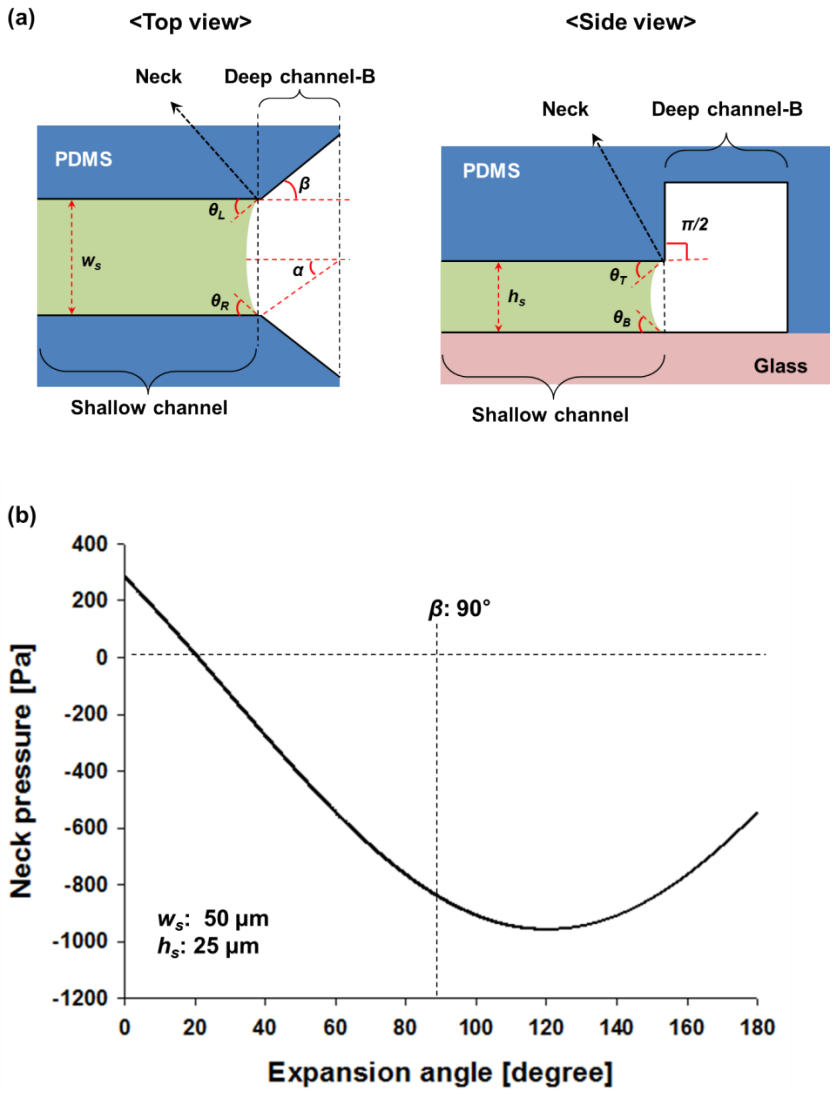

Fig. S3 (a) Schematic of the capillary flow of diluted nanoparticles at the neck of the shallow channel. (b) Theoretical neck pressure, P_n, by varying the expansion angle, β.

The diluted nanoparticles at the intersection between shallow and deep channel experience a sudden pressure drop (ΔP_{12}), which tries to drag the solution in the deep channel into the shallow channel ($F_{shallow}$).[3] When this flow of solution in shallow channel is located at the neck (interface between shallow channel and deep channel-B, **Fig. S3(a)**), the capillary pressure at the neck (P_n) is induced and it can be expressed as below:[4]

$$P_n = \delta(\frac{\sin\alpha}{\alpha}) \times (\frac{\cos(\theta_T + \pi/2) + \cos\theta_B}{h_s} + \frac{\cos(\theta_L + \beta) + \cos(\theta_R + \beta)}{w_s}) \quad \text{(S1)}$$

here, δ, h_s, and w_s is the surface tension, the height of shallow channel, and the width of shallow channel, respectively. θ is the contact angle and the subscripts T, B, L, and R indicate the top, bottom, left and right surface of the shallow channel, respectively. α is the curvature angle and β is the expansion angle in the width direction. In these equations, the solution may move forward toward the deep channel-B when the capillary pressure at the neck, P_n, is positive, and stop at the neck when P_n is negative. **Fig. S3(b)** shows the change of P_n as varying the expansion angle. The width (w_s) and height (h_s) of the shallow channel was 50 μm and 25 μm, respectively. The value of the surface tension with 0.025 N/m was used for 70 % of the ethanol,[5] and the contact angles were measured from the PDMS substrate (for θ_T, θ_L, and θ_R, ~60°) and glass substrate (for θ_B, ~45°). The negative P_n (stop pressure at the neck) are maximized at β around the 120° and still negative at 90° of the β. Therefore the capillary stop pressure at the neck is induced and the solution could not move forward toward the deep channel-B.

<Fig. S2(d)>

After the solution stop at the neck, the evaporation of the solvent (70 % of the ethanol) is induced through the deep channel-B. Then the solvent with the convective transport of nanoparticles is introduced from the deep channel-A toward the neck to compensate of the solvent loss by evaporation. This influx of the nanoparticles promotes the growth of the

ordered lattice (FCC structure) from neck to the deep channel-A in unidirectional. However, the careful selection of the size of the nanoparticles and the control of the Debye length, λ_D (it can be controlled by change of the material or ionic strength, and pH) are required because if the nanoparticles have strong repulsive interactions, the assembly to non-FCC structure can happen.[6] When the effective diameter (d_{eff}) of the spheres containing Debye length is close to or larger than the center-to-center distance (d_c) between two spheres ($d_{eff} = d + 2\lambda_D > d_c$, wherein d is the diameter of the colloidal spheres), the colloidal spheres act like "hard spheres" and they will not influence each other until they are in physical contact.[6, 7] In this case, the FCC crystal structure is formed, and no heat or energy change is involved upon crystallization.

<Fig. S2(e) and (f)>

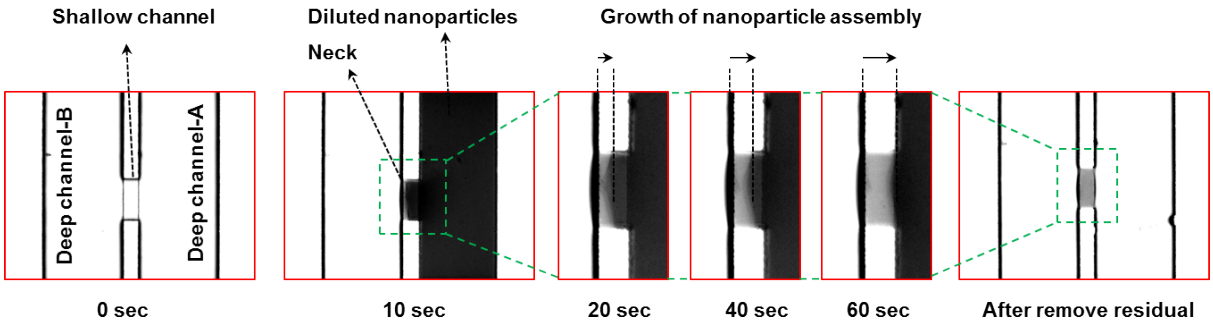

Fig. S4 Time sequence microscopic images of the in situ formation of nanochannel networks membrane using nanoparticles.

(e) When the growth of the nanoparticle assembly reaches the interface between the shallow channel and deep channel-A, the residual solution in deep channel-A is gently removed. Here, the growth of the nanoparticle assembly is easily observed by monitoring the change of the contrast of the light in the shallow channel through the inverted microscope (IX7, Olympus

Co., Tokyo, Japan) as shown in **Fig. S4**. **(f)** Finally, self-assembled nanoparticles are dried out in room temperature for one day.

S.III Effective cross sectional area of ideally close-packed homogeneous nanoparticles into the FCC structure[8]

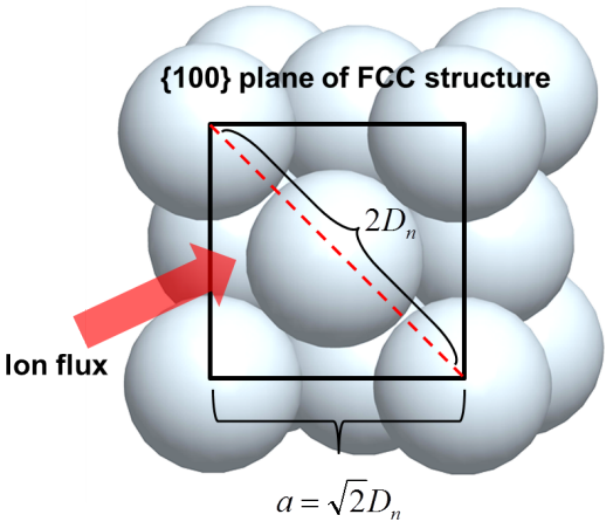

Fig. S5 Effective cross sectional area of ideally close-packed homogeneous nanoparticles into the FCC structure

This section is followed our previous report.[8] Fig. S5 shows a unit of the effective cross section area (A_u^*) of the ideally close-packed homogeneous nanoparticles on the {100} plane of the FCC structure. A_u^* can be described as follows:

$$A_u^* = a^2 - 2\pi(\frac{D_n}{2})^2 \qquad \text{(S2)}$$

here, the former term, a^2, is the unit of the cross sectional area of the {100} plane and the latter term is the unit of the cross sectional area of the closed packed particles within the {100} plane. As substituting the $a = \sqrt{2}D_n$ for eqn. S2, the A_u^* becomes following expressions:

$$A_u^* = (\sqrt{2}D_n)^2 - 2\pi(\frac{D_n}{2})^2 \approx 0.43{D_n}^2 \approx 0.215a^2 \qquad \text{(S3)}$$

Since the close-packed nanoparticle with FCC structure has the same packing efficiency, the ratio is insensitive to the width (w_s) and the height (h_s) of the shallow channel. In this reason, the effective cross sectional area of the shallow channel, A_s^*, can be estimated as $A_s^* = 0.215 w_s h_s$, i.e. 21.50 % of the A_s.

REFERENCE

1. E. Choi, H. K. Chang, C. Y. Lim, T. Kim and J. Park, *Lab Chip*, 2012, 12, 3968-3975.
2. E. Choi, K. Kwon, D. Kim and J. Park, *Lab Chip*, 2015, 15, 168-178.
3. S. Chung, H. Yun and R. D. Kamm, *Small*, 2009, 5, 609-613.
4. K. H. Chung, J. W. Hong, D.-S. Lee and H. C. Yoon, *Anal. Chim. Acta*, 2007, 585, 1-10.
5. G. Vazquez, E. Alvarez and J. M. Navaza, *J. Chem. Eng. Data*, 1995, 40, 611-614.
6. Y. N. Xia, B. Gates, Y. D. Yin and Y. Lu, *Adv. Mater.*, 2000, 12, 693-713.
7. T. Okubo, *Langmuir*, 1994, 10, 1695-1702.
8. E. Choi, K. Kwon, D. Kim and J. Park, *Lab Chip*, 2015, 15, 512-523.